

Reaction of Nitromethane with an Iridium Pincer Complex. Multiple Binding Modes of the Nitromethanate Anion

Xiawei Zhang, Thomas J. Emge, Rajshekhar Ghosh, Karsten Krogh-Jespersen,* and Alan S. Goldman*

Department of Chemistry and Chemical Biology, Rutgers, The State University of New Jersey, New Brunswick, New Jersey 08903

Received July 30, 2005

The reaction of nitromethane with (PCP)Ir (PCP = κ^3 -2,6-(^tBu₂PCH₂)₂C₆H₃) yields the bidentate O,O-ligated nitromethanate complex (PCP)Ir(H)(κ^2 -O,O-NO₂CH₂) (**1**). Reaction of **1** with CO affords a CO adduct with a mono-oxygen-ligated nitromethanate, **2**, which represents the first characterized transition metal mono-oxygen-ligated nitromethanate complex. At elevated temperature, complex **2** isomerizes to give the carbon-bound nitromethyl complex **3**. Complex **1** also undergoes addition of cyclohexylisocyanide (analogous to the reaction with CO) to form the mono-oxygen-ligated nitromethanate complex **4**, which also isomerizes to form the corresponding nitromethyl complex, **5**. The (PCP)Ir-(CH₃NO₂) system is the first species known to display three binding modes with a nitromethanate anion. Results from density functional calculations illustrate the structures and energies of the minima and transition states on the potential energy surfaces. The calculations suggest that **1** is the thermodynamic product of (PCP)Ir reacting with nitromethane; a kinetic product, formed via oxidative addition of a nitromethane C–H bond, should readily rearrange to form **1**.

Introduction

The inorganic and organometallic chemistry of nitroalkanes has long been of interest. In recent years, metal-mediated reactions of nitromethane have seen increasing applications in organic synthesis. Aldol-type reactions have made accessible a large number of new nitro alcohols and nitro glycols, which in turn can be transformed into valuable building blocks.^{1–3} In the past several years, the development of catalysts for asymmetric nitroaldol (Henry) reactions has been a particularly active area.^{4–6}

Coordinated nitroalkanate ions, most commonly nitromethanate, are the putative active species in reactions such as the metal-catalyzed nitroaldol and related reactions. The nitromethanate anion can bind in several different coordination modes. Nitromethanate complexes with bidentate coordination through the two oxygen atoms^{7–16} or monodentate coordination of one

carbon atom^{17–23} have been isolated and characterized with different transition metal systems. In most such cases, base was used to deprotonate the nitroalkane and to promote the coordination. The structure proposed for the key nitromethanate intermediates in the transition metal-catalyzed nitroaldol reactions is monodentate oxygen-bound.^{4–6} However, no monodentate oxygen-bound complexes have been previously isolated and characterized.

Pincer-ligated transition metal complexes are currently the subject of intense study.^{24–26} The 14-electron species (PCP)Ir (PCP = κ^3 -2,6-(^tBu₂PCH₂)₂C₆H₃), generated from (PCP)IrH₂, can readily cleave hydrocarbon C–H bonds,²⁷ activate the O–H bond in water,²⁸ and oxidatively add N–H bonds of anilines.²⁹ In this context, we have been investigating the reactivity of

* To whom correspondence should be addressed. E-mail: agoldman@rutchem.rutgers.edu; krogh@rutchem.rutgers.edu.

- (1) Luzio, F. A. *Tetrahedron* **2001**, *57*, 915.
- (2) *The Nitro Group in Organic Synthesis*; Ono, N., Ed.; Wiley-VCH: New York, 2001; 392 pp.
- (3) Seebach, D.; Beck, A. K.; Mukhopadhyay, T.; Thomas, E. *Helv. Chim. Acta* **1982**, *65*, 1101.
- (4) Palomo, C.; Oiarbide, M.; Mielgo, A. *Angew. Chem., Int. Ed.* **2004**, *43*, 5442–5444.
- (5) (a) Trost, B. M.; Yeh, V. S. C. *Angew. Chem., Int. Ed.* **2002**, *41*, 861–863. (b) Trost, B. M.; Yeh, V. S. C.; Ito, H.; Bremeyer, N. *Org. Lett.* **2002**, *4*, 2621–2623.
- (6) Evans, D. A.; Seidel, D.; Rueping, M.; Lam, H. W.; Shaw, J. T.; Downey, C. W. *J. Am. Chem. Soc.* **2003**, *125*, 12692–12693.
- (7) Balogh-Hergovich, É.; Gréczy, Z.; Kaizer, J.; Speier, G.; Réglér, M.; Giorgi, M.; Párkányi, L. *Eur. J. Inorg. Chem.* **2002**, 1687.
- (8) Diel, B. N.; Hope, H. *Inorg. Chem.* **1986**, *25*, 4448.
- (9) Ito, H.; Ito, T. *Chem. Lett.* **1985**, 1251.
- (10) Kovács, T.; Speier, G.; Réglér, M.; Giorgi, M.; Vértes, A.; Vankó, G. *Chem. Commun.* **2000**, 469.
- (11) Balogh-Hergovich, E.; Speier, G.; Huttner, G.; Zsolnai, L. *Inorg. Chem.* **1998**, *37*, 6535.
- (12) Kubota, M.; Yamamoto, A. *Bull. Chem. Soc. Jpn.* **1978**, *51*, 2909.

(13) Camus, A.; Marsich, N.; Nardin, G.; Randaccio, L. *J. Chem. Soc., Dalton Trans.* **1975**, 2560.

(14) Cook, J. A.; Drew, M. G. B.; Rice, D. A. *J. Chem. Soc., Dalton Trans.* **1975**, 1973.

(15) Simonsen, O. *Acta Crystallogr.* **1973**, *B29*, 2600.

(16) Yamamoto, T.; Kubota, M.; Miyashita, A.; Yamamoto, A. *Bull. Chem. Soc. Jpn.* **1978**, *51*, 1835.

(17) Davis, J. A.; Dutremez, S.; Pinkerton, A. A.; Vilmer, M. *Organometallics* **1991**, *10*, 2956.

(18) Akiba, M.; Sasaki, Y. *Inorg. Chem. Commun.* **1998**, *1*, 61.

(19) Milani, B.; Corso, G.; Zangrando, E.; Randaccio, L.; Mestroni, G. *Eur. J. Inorg. Chem.* **1999**, 2085.

(20) Randaccio, L.; Bresciani-Pahor, N.; Toscano, P. J.; Marzilli, L. G. *Inorg. Chem.* **1981**, *20*, 2722.

(21) Murata, K.; Konishi, H.; Ito, M.; Ikariya, T. *Organometallics* **2002**, *21*, 253.

(22) Cairns, M. A.; Dixon, K. R.; Smith, M. A. R. *J. Organomet. Chem.* **1977**, *135*, C33.

(23) Randaccio, L.; Bresciani-Pahor, N.; Toscano, P. J. *Inorg. Chem.* **1981**, *20*, 2722.

(24) Albrecht, M.; van Koten, G. *Angew. Chem., Int. Ed.* **2001**, *40*, 3750–3781, and references therein.

(25) van der Boom, M. E.; Milstein, D. *Chem. Rev.* **2003**, *103*, 1759–1792.

(26) Singleton, J. T. *Tetrahedron* **2003**, *59*, 1837–1857.

(27) Kanzelberger, M.; Singh, B.; Czerw, M.; Krogh-Jespersen, K.; Goldman, A. S. *J. Am. Chem. Soc.* **2000**, *122*, 11017–11018.

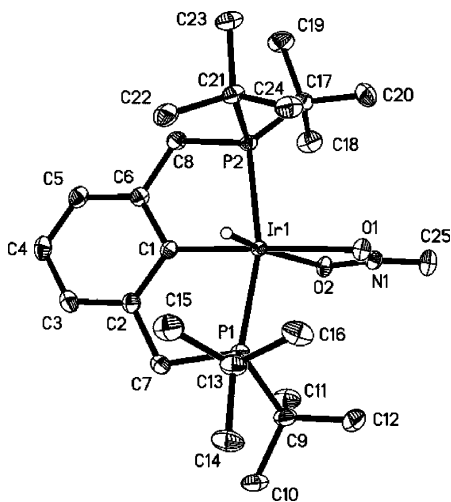


Figure 1. X-ray structure of complex **1**.

pincer-iridium complexes toward various classes of organic molecules. Herein, we report the formation of three iridium pincer complexes from the reaction of (PCP)Ir with nitromethane; each complex formed features a different binding mode of the nitromethanate ligand. Reaction mechanisms are proposed on the basis of results from DFT calculations.

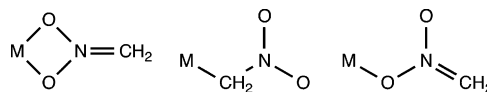
Experimental Results

Formation of (PCP)Ir(H)(κ^2 -O,O-NO₂CH₂) (1**).** The reaction of the 16-electron species (PCP)IrH₂ with norbornene in *p*-xylene solution is known to generate a precursor of the highly active 14-electron species (PCP)Ir(I).³⁰ When nitromethane (2 equiv) is added to a *p*-xylene solution of (PCP)IrH₂ in the presence of excess norbornene, the red solution turns a dark blue. The same initial color change is observed upon addition of nitrobenzene or 2-methyl-2-nitropropane. In accord with electronic structure calculations discussed in the next section of this paper, we believe that these dark blue species are simple O-bound nitroalkane (or nitroarene) complexes.

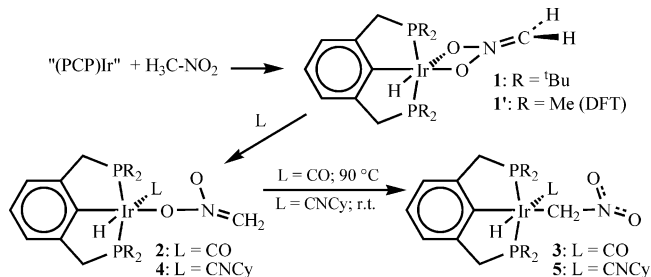
Within 10 s, the dark blue solution turns yellow and NMR reveals formation of a new complex, **1**, in quantitative yield (³¹P{¹H} NMR: δ 59.16 ppm, d, $J_{\text{PH}} = 12.8$ Hz). The NMR data for **1** are consistent with its formulation as a six-coordinate (PCP)Ir(III) complex with a hydride *trans* to a low-field ligand (e.g., a coordinating oxygen atom; δ -29.32 ppm, t, $J_{\text{PH}} = 13.5$ Hz). At room temperature, the ¹H NMR spectrum shows a broad singlet at δ 5.01 ppm with an integrated peak area of 2 H. However, at lower temperature (< ca. 0 °C) an AB pattern is observed, consistent with the presence of two inequivalent, coupled, methylene protons. The IR spectrum of the pentane solution of **1** shows an intense absorption at 1575 cm⁻¹, consistent with $\nu_{(\text{C}=\text{N})}$ values of previously reported κ^2 -nitroalkane complexes.^{7,9,10,16} A signal at δ 100.1 ppm (s) in the ¹³C NMR spectrum is attributable to the nitromethanate ligand.

Complex **1** was crystallized from pentane solution. A single-crystal X-ray structure determination of **1** (Figure 1) reveals a distorted octahedral geometry around the iridium atom with a bidentate O,O-bound nitromethanate ligand; a hydride ligand was located *trans* to one of the oxygen atoms (see Scheme 2).

Scheme 1. Binding Modes in Metal Nitromethanate Complexes



Scheme 2. Species Isolated from the Reaction of (PCP)Ir with Nitromethane



Selected bond distances and bond angles are listed in Table 1.³¹ The nitromethanate ligand and the iridium atom are coplanar. The C–N distance is 1.294(2) Å, about typical for that of an oxime.³² The two N–O bond distances are nearly identical (1.3235(18) and 1.3288(19) Å); a comparison with the N–O bond distances in oximes (1.36–1.42 Å) and nitro compounds (1.22–1.25 Å)³² indicates that the N–O bonds of **1** are of predominantly, but not exclusively, single-bond character. Three resonance forms may be readily considered for the nitromethanate anion (Scheme 3). On the basis of considerations noted above, the bond lengths and angles of the nitromethanate ligand in complex **1**, as well as the spectral properties, correlate best with resonance structure **a**; the short N–O distances suggest some contribution of structure **b**.

Reaction of **1 with CO.** Complex **1** reacted readily with CO (800 Torr); a bright yellow *p*-xylene solution rapidly turned pale yellow. Evaporation of solvent yielded a pale yellow solid, **2** (98% yield), which was characterized by NMR and IR spectroscopy and X-ray crystallography. In the selectively decoupled ³¹P NMR spectrum, complex **2** resonates at δ 58.22 ppm as a doublet ($J_{\text{PH}} = 13.9$ Hz). In the ¹H NMR spectrum, a hydride signal appears as a triplet at δ -7.43 ppm ($J_{\text{PH}} = 13.5$ Hz), within the usual range for hydrides *trans* to a CO ligand in six-coordinate (PCP)Ir(III) complexes (approximate range -7 to -12 ppm). A broad singlet at δ 6.01 ppm with an integral of 2 H sharpens to an AB pattern below room temperature in a manner similar to the behavior of complex **1**, suggesting that the nitromethanate structure is preserved in the CO adduct **2**. A signal at δ 93.4 ppm (s) in the ¹³C NMR spectrum is assigned to the nitromethanate ligand; this is 7 ppm upfield from the corresponding signal in **1**. A strong absorption at 2004 cm⁻¹ in the IR spectrum is clearly attributable to the CO ligand. A second strong absorption at 1547 cm⁻¹ is probably due to the stretching mode of a weakened C–N bond (cf. 1575 cm⁻¹ for **1**). Thus, the spectroscopic data are consistent with the formulation of **2** as a six-coordinate complex with CO and a κ^1 -O-nitromethanate ligand coordinated to iridium.

A single-crystal X-ray structure determination of **2** (Figure 2) confirms the structure of the complex inferred from IR and NMR spectroscopy. Selected bond distances and bond angles are given in Table 1.³¹ Complex **2** has an approximately octahedral geometry around the iridium atom with a monoden-

(28) Morales-Morales, D.; Lee, D. W.; Wang, Z.; Jensen, C. M. *Organometallics* **2001**, *20*, 1144–1147.

(29) Kanzelberger, M.; Zhang, X.; Emge, T. J.; Goldman, A. S.; Zhao, J.; Incarvito, C.; Hartwig, J. F. *J. Am. Chem. Soc.* **2003**, *125*, 13644–13645.

(30) Zhang, X.; Kanzelberger, M.; Emge, T. J.; Goldman, A. S. *J. Am. Chem. Soc.* **2004**, *126*, 13192–13193.

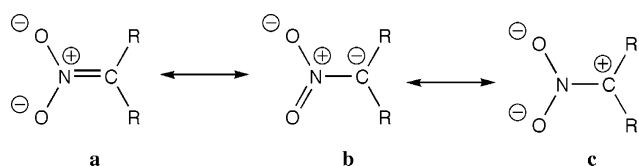
(31) See Supporting Information for experimental details and procedures, and spectroscopic and crystallographic data.

(32) See ref 11 and refs 30 and 31 therein.

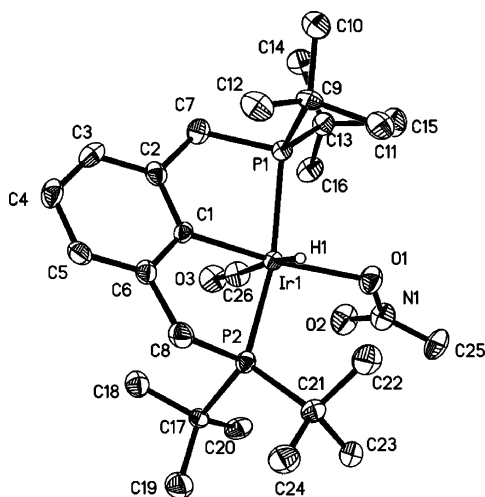
Table 1. Selected Bond Distances (Å) and Angles (deg) for Nitromethane Complexes 1–3 and 5³¹

	1 (κ^2 -O,O-bound)	2 (κ^1 -O-bound)	3 (κ^1 -C-bound)	5 (κ^1 -C-bound)
Ir(1)–C(1)(PCP)	2.0283(17)	2.042(6)	2.091(3)	2.090(2)
Ir(1)–O(1)	2.1952(12)	2.148(5)		
Ir(1)–O(2)	2.2540(12)			
Ir(1)–P(1)	2.3117(5)	2.3325(16)	2.3447(9)	2.3374(5)
Ir(1)–P(2)	2.3185(5)	2.3349(16)	2.3499(9)	2.3399(5)
Ir(1)–H(1)	1.518(16)	1.78(2)	1.531(18)	1.574(16)
Ir(1)–C(25)(CH ₂ NO ₂)			2.194(4)	2.209(2)
N(1)–C(25)	1.294(2)	1.307(9)	1.448(5)	1.445(3)
N(1)–O(2)	1.3235(18)	1.261(8)	1.225(5)	1.229(3)
N(1)–O(1)	1.3288(19)	1.361(7)	1.229(5)	1.233(3)
Ir(1)–C(26)(CO or CNR)		1.914(6)	1.911(4)	1.997(2)
O(3)–C(26)		1.154(8)	1.144(4)	
C(1)–Ir(1)–O(1)	175.20(6)	169.3(2)		
C(1)–Ir(1)–C(25)			168.77(14)	170.21(8)
C(1)–Ir(1)–H(1)	78.6(10)	87(3)	84.6(14)	86.1(10)
O(1)–Ir(1)–H(1)	106.1(10)	84(3)		
C(26)–Ir(1)–C(1)		90.9(3)	92.06(14)	95.86(8)
O(2)–Ir(1)–H(1)	165.6(10)			
P(1)–Ir(1)–P(2)	162.218(16)	158.78(6)	158.37(3)	158.004(19)
O(2)–N(1)–O(1)	112.72(13)	119.2(5)	121.7(4)	121.5(2)
C(25)–N(1)–O(1)	123.41(16)	115.6(6)	118.7(4)	119.1(2)
O(2)–N(1)–C(25)	123.88(16)	125.2(6)	119.5(4)	119.3(2)
C(25)–N(1)–O(1)–Ir(1)	176.90(16)	–153.9(6)		
O(2)–N(1)–O(1)–Ir(1)	–2.81(14)	27.8(9)		
O(1)–N(1)–C(25)–Ir(1)			–95.5(4)	80.0(3)

Scheme 3. Resonance Forms of the Nitromethane Anion



tate oxygen-coordinated nitromethane ligand and a CO ligand *trans* to a hydride. Relative to complex **1**, one coordinating oxygen atom of the CH₂NO₂[–] ligand has been displaced by the CO molecule. The remaining oxygen binds to iridium with a bond shorter (2.148(5) Å) than those observed in **1** (2.1952(12) and 2.2540(12) Å, respectively). The nitromethane ligand remains coplanar. The C–N distance (1.307(9) Å) in **2** is slightly longer than that in complex **1** (1.294(2) Å), while the two N–O bonds are distinctly inequivalent (N–O(1) = 1.361(7) Å, N–O(2) = 1.261(8) Å) and on average slightly shorter than those in **1**. The N–O(1) (oxygen bound to iridium) bond is slightly longer than the N–O bond in complex **1** (ca. 1.326 Å), indicating that the N–O(1) bond in complex **2** is essentially a single bond, while the shorter N–O(2) bond distance in **2** is close to that typical of N–O double bonds. Thus, relative to

Figure 2. X-ray structure of complex **2**.

complex **1**, the nitromethane ligand in complex **2** appears to have slightly more character of resonance structure **b** (although still predominantly **a** in character) with the negatively charged oxygen bound to iridium (Scheme 3). The slightly upfield ¹³C NMR resonance of the nitromethane carbon, relative to **1**, also seems consistent with this resonance interpretation. An analogous conversion of (PCP)Ir-coordinated bicarbonate from bidentate oxygen coordination to mono-oxygen coordination has been reported by Jensen and co-workers.³³

To the best of our knowledge, complex **2** is the first characterized transition metal complex with a mono-oxygen-coordinated nitroalkane ligand. The closest reported precedents are mono-oxygen-coordinated phenylnitromethane alkali metal complexes.³⁴ The apparent contribution of resonance form **b** may be important in the context of aldol-type reactions, where a putative mono-oxygen-coordinated nitroalkane acts as a carbon nucleophile.^{5,6}

Upon heating under CO atmosphere in *p*-xylene solution at 90 °C for 24 h, complex **2** was converted to complex **3** in 75% yield with some additional formation of four-coordinate (PCP)Ir(CO). A doublet at δ 50.08 ppm appears in the selectively decoupled ³¹P NMR spectrum of complex **3**. In the ¹H NMR, a signal at δ –9.61 ppm (t, $J_{\text{PH}} = 15.8$ Hz) is indicative of a hydride ligand bound to six-coordinate (PCP)Ir(III). A triplet at δ 5.61 ppm ($J_{\text{PH}} = 5.0$ Hz) with an integral of 2 H may be assigned to a C-bound nitromethyl group. The ¹³C NMR spectrum of **3** reveals a triplet at δ 32.9 ppm ($J_{\text{CP}} = 4.5$ Hz), attributable to the nitromethyl group; this is upfield by over 60 ppm from the nitromethane signals (singlets) in **1** and **2**. This upfield value is in excellent agreement with the only other ¹³C NMR data reported, to our knowledge, for a (nitromethyl)iridium complex: δ 36.7 ppm for the chemical shift of the nitromethyl carbon of Cp^{*}Ir(CH₂NO₂)[(R,R)-Tscyd].³⁵ The IR spectrum of the benzene solution of **3** shows intense absorptions at 1498

(33) Lee, D. W.; Jensen, C. M.; Morales-Morales, D. *Organometallics* **2003**, *22*, 4744–4749.

(34) (a) Boche, G.; Marsch, M.; Massa, W.; Baum, G.; Klebe, G.; Boehn, K. H.; Harms, K.; Sheldrick, G. M. *Stud. Org. Chem. (Amsterdam)* **1987**, *31*, 149. (b) Klebe, G.; Boehn, K. H.; Marsch, M.; Boche, G. *Angew. Chem.* **1987**, *99*, 62.

(35) Murata, K.; Konishi, H.; Ito, M.; Ikariya, T. *Organometallics* **2002**, *21*, 253–255.

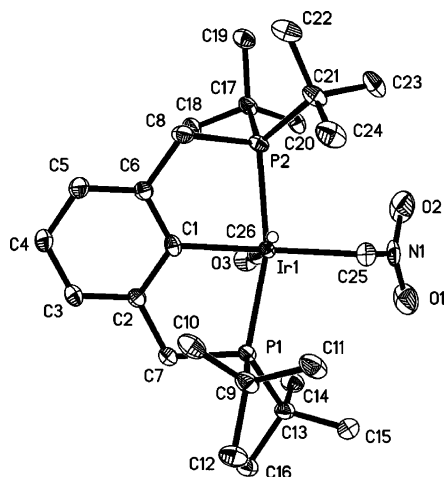


Figure 3. X-ray structure of complex **3**.

and 1355 cm^{-1} , attributable to asymmetric and symmetric stretches of the NO_2 group, respectively. A strong IR absorption band at 1988 cm^{-1} is assigned to the CO group.

A single-crystal X-ray structure determination of complex **3**, crystallized from benzene solution, reveals a distorted octahedral geometry around the iridium atom with a C-bound nitromethyl ligand located *trans* to the PCP phenyl carbon (Figure 3 and Table 1). The C–N bond distance, $1.448(5)\text{ \AA}$, is much longer than that of **1** or **2** (ca. $1.30 \pm 0.01\text{ \AA}$) and indicative of a single bond (1.47 \AA). The two N–O bonds ($1.225(5)$ and $1.229(5)\text{ \AA}$) are typical of an uncoordinated nitro group ($1.22\text{--}1.25\text{ \AA}$).

Reaction of 1 with Isocyanide. Complex **1** displayed reactivity with isocyanide analogous to that observed with CO. When a small excess of cyclohexylisocyanide was added to a solution of **1**, the yellow solution quickly turned pale yellow. Complex **4** was formed and was characterized by $^{31}\text{P}\{^1\text{H}\}$ and ^1H NMR spectroscopy. In the selectively decoupled ^{31}P NMR spectrum, complex **4** resonates at $\delta\ 57.40\text{ ppm}$ as a doublet. In the ^1H NMR spectrum, there is a hydride triplet at $\delta\ -9.35\text{ ppm}$ (t, $J_{\text{PH}} = 15.9\text{ Hz}$). The methylene protons of the nitromethyl ligand resonate at $\delta\ 5.96\text{ ppm}$ as a broad singlet. All the spectroscopic data are consistent with a structure analogous to the CO complex **2** in which the nitromethyl group coordinates to iridium with one oxygen atom, while the isocyanide ligand occupies the position *trans* to the hydride. Crystallization of complex **4** was not successful.

At room temperature in *p*-xylene solution, complex **4** isomerized to **5** over a period of several hours. Complex **5** was characterized by NMR spectroscopy and a single-crystal X-ray structure determination. The NMR spectral characteristics of **5** are very similar to those of complex **3**. The X-ray crystal structure of **5** (Figure 4 and Table 1)³¹ confirms a structure analogous to that of the C-bound nitromethyl complex **3**.

Computational Results and Discussion

Electronic structure calculations at the DFT level (see Computational Details) were carried out to further illustrate the minima and transition states on the potential energy surfaces for species **1–5**. To computationally model the pincer ligand, the bis(dimethylphosphino) analogue of PCP ($(\text{Me}_2\text{PCH}_2)_2\text{C}_6\text{H}_3$, PCP') was used for all calculations in this work.

Tautomerization Prior to Addition. A priori, plausible pathways for the formation of **1** include C–H addition to (PCP)–Ir, followed by ligand rearrangement, or O-coordination of nitromethane followed by proton transfer to iridium. A seem-

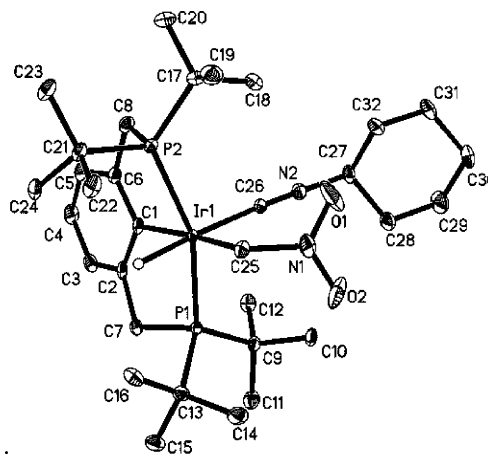
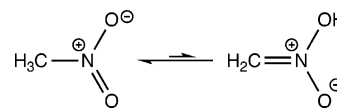


Figure 4. X-ray structure of complex **5**.

ingly less likely pathway might involve O–H activation from nitronic acid, the tautomer of nitromethane.



The computed free energy difference between nitromethane and nitronic acid is 13.8 kcal/mol in favor of nitromethane, implying an equilibrium constant in the gas phase of $K_{\text{eq}} \approx 10^{-10}$ ($T = 300\text{ K}$). The computed free energy barrier for the intramolecular 1,3-H shift is 53.4 kcal/mol . Thus, in accord with conclusions derived from previous calculations,³⁶ the presence of (or reactions involving) nitronic acid does not need to be considered further given the reaction conditions employed in this study.

Nitromethane Complexes. Considering the unsaturated nature of the reactive metal complex, the formation of precursor complexes between the reactants, (pincer)Ir and CH_3NO_2 , should be quite favorable. Indeed, a four-coordinate complex, (PCP')–Ir(O_2NCH_3) (**6a'**), in which both oxygen atoms point toward the Ir atom but only one is coordinating (Ir–O1 = 2.091 \AA , Ir–O2 = 3.368 \AA , N–O1 = 1.298 \AA , N–O2 = 1.259 \AA , C–N = 1.478 \AA , Ir–O1–N–O2 = 5.2°) was readily located with a free energy 14.5 kcal/mol below that of the isolated reactants ($\Delta H_{\text{binding}} = 24.7\text{ kcal/mol}$). A second complex (**6b'**), also featuring κ^1 -O binding (Ir–O1 = 2.150 \AA , Ir–O2 = 4.293 \AA , Ir–C = 3.410 \AA , N–O1 = 1.288 \AA , N–O2 = 1.249 \AA , C–N = 1.488 \AA , Ir–O1–N–O2 = 170.8°) and possibly a very weak C–H α -agostic interaction (C–H $_{\alpha}$ = 1.106 \AA , remaining C–H $\approx 1.101\text{ \AA}$; Ir–H $_{\alpha}$ = 2.785 \AA), was located 6.3 kcal/mol above this complex ($\Delta G_{\text{binding}} = 8.2\text{ kcal/mol}$, $\Delta H_{\text{binding}} = 18.4\text{ kcal/mol}$). We were not successful in locating a (PCP)Ir–nitromethane complex with κ^2 -O,O binding clearly involving both oxygen atoms; all trial structures with bidentate O,O interactions rearranged upon geometry optimization to a structure showing only κ^1 -O binding (**6a'** or **6b'**). In **6b'**, the nitromethane unit is lying in the “equatorial plane” (the plane bisecting the P–Ir–P axis) of the pincer-iridium complex, whereas in **6a'** the nitromethane species is oriented approximately in the “vertical plane” (the plane containing the P–Ir–P axis and, approximately, the PCP aryl group). The actual (PCP)Ir complex (with P^iBu_2 rather than P^iMe_2 groups) offers a cleft for small molecules oriented approximately in the equatorial plane, and the presence

(36) Lammertsma, K.; Prasad, B. V. *J. Am. Chem. Soc.* **1993**, *115*, 2348–51.

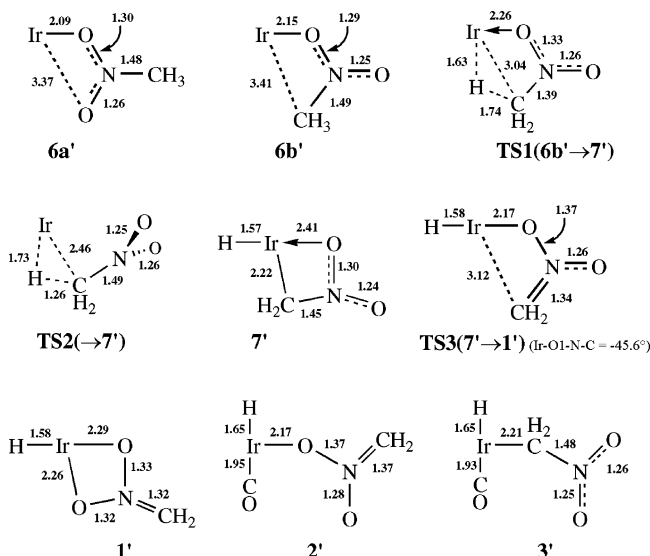


Figure 5. Schematic illustration of bond lengths in selected calculated complexes.

of *tert*-butyl groups would therefore be expected to significantly raise the energy of **6a'** relative to **6b'**.

Experimentally, as noted above in the first section, the reaction of "(PCP)Ir" with nitromethane, or with nitrobenzene or 2-methyl-2-nitropropane, results in the appearance of a very short-lived dark blue color. It appears very plausible that these dark blue species are nitro-O-bound adducts, analogous to calculated models **6a'** and/or **6b'**.

Nitromethanate Complexes. Two (PCP)Ir-hydride-nitromethanate complexes were located computationally: the κ^2 -O,O-coordinated species, **1'** (Ir–O1 = 2.258 Å, Ir–O2 = 2.295 Å, C–N = 1.324 Å; the analogue of the isolated complex **1**) and a species coordinating primarily through the C atom with some additional binding via one O atom (**7'**; Ir–C = 2.225 Å, Ir–O1 = 2.408 Å, C–N = 1.454 Å) (see Scheme 4). The free energy of species **1'** is 6.1 kcal/mol less than that of species **7'** and 8.7 kcal/mol less than the free energy of the most stable precursor complex (**6a'**). The computed C–N stretching frequency of **1'** is 1573.5 cm⁻¹, exceedingly close to the frequency of 1575 cm⁻¹ observed in **1**.

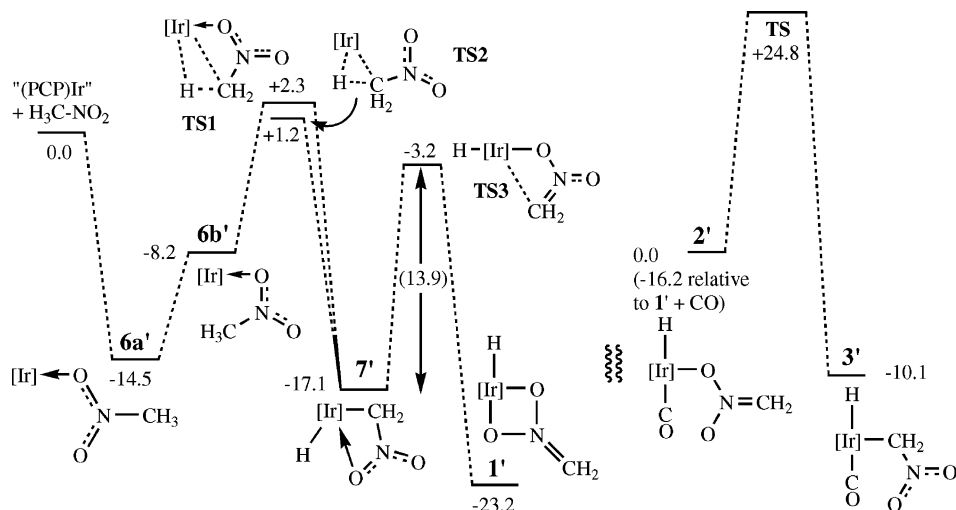
Starting with κ^1 -O bound **6b'** as the reactant, a transition state for C–H bond breaking was located with $\Delta G^\ddagger = 10.5$ kcal/

mol (only 2.3 kcal/mol above the total free energy of (PCP)Ir and CH₃NO₂). Intrinsic reaction coordinate (IRC) calculations verified that this transition state (**TS1**, Scheme 4) connects **6b'** to C-bound **7'**. The TS geometry shows that the Ir–H bond is almost fully formed and the C–H bond fully broken while Ir–O1 bonding is mostly maintained (Ir–H = 1.633 Å, C–H = 1.737 Å, Ir–O1 = 2.259 Å, Ir–C = 3.040 Å, C–N = 1.388 Å, Ir–O2 = 4.022 Å, N–O1 = 1.330 Å, N–O2 = 1.255 Å, Ir–C–N–O1 = -27.8°). A second TS (**TS2**, Scheme 4), also leading to **7'** as the product, was located only 1.2 kcal/mol above the isolated (PCP)Ir and CH₃NO₂ reactants. In this TS, C–H activation occurs in a nitromethane molecule oriented "face-on" to the Ir atom with the C–N bond lying in the horizontal plane and the oxygen atoms pointing toward the phosphino alkyl groups (Ir–H = 1.733 Å, C–H = 1.259 Å, Ir–C = 2.464 Å, C–N = 1.489 Å, Ir–O1 = 3.469 Å, Ir–O2 = 3.500 Å, N–O1 = 1.252 Å, N–O2 = 1.259 Å, Ir–C–N–O1 = 90.1°). Thus, nitromethane C–H addition is calculated to be facile either with or without concomitant binding to an O atom, although the presence of *tert*-butyl groups on phosphorus would be expected to selectively raise the energy of the second TS.

We have not found a direct route to the formation of **1'** from a nitromethane precursor in our calculations, and the κ^2 -O,O-coordinated species **1** is most likely formed from a C-bound species analogous to **7'**. The computed activation energy for the intramolecular migration of the nitromethanate ligand (7' → **1'**) is only $\Delta G^\ddagger = 13.9$ kcal/mol (**TS3**, Scheme 4). IRC calculations and visual examination of the reaction coordinate at **TS3** shows that the nitromethanate species pivots around the Ir–O1 linkage, which is maintained throughout the migration. The Ir–O1 bond length is very short in **TS3** (Ir–O1 = 2.171 Å versus 2.408 Å in **7'** and 2.258 Å in **1'**; N–O1 = 1.372 Å, Ir–O1–N–C = -45.6°), and there appears to be no particular metal interaction with the C atom (Ir–C = 3.120 Å) or with the other O atom (Ir–O2 = 3.995 Å), which is essentially doubly bonded to the N atom, cf. resonance form **b** in Scheme 3 (N–O2 = 1.258 Å, C–N = 1.343 Å). On the basis of these calculations, we thus suggest that the observed species **1** is the thermodynamic product of (PCP)Ir reacting with nitromethane, while a precursor with a C-bound nitromethanate ligand rearranges to **1** too rapidly to be isolated.

The two CO-containing complexes, **2'** and **3'**, are computed to be separated by $\Delta G = 10.1$ kcal/mol, in favor of C-bound

Scheme 4. Calculated Free-Energy Values (kcal/mol) for Various Nitromethane and Nitromethanate Complexes and Transition States ([Ir] = (PCP)Ir)



species **3'**. The formation reaction for **2'** from CO and **1'** is computed to be moderately exothermic ($\Delta H = -25.6$ kcal/mol, $\Delta G = -16.2$ kcal/mol). In **2'**, the calculations predict the (unscaled) C–N and C–O stretch frequencies at 1524 and 1956 cm^{-1} , respectively, in good agreement with the observed frequencies (1547 and 2004 cm^{-1}). In **3'**, the calculations predict the N–O symmetric and asymmetric stretch frequencies at 1344 and 1524 cm^{-1} , respectively, and the C–O stretch frequency at 1959 cm^{-1} , again in good agreement with the observed frequencies (1355, 1498, and 1988 cm^{-1}). The transition state for intramolecular rotation of nitromethanate, leading to interconversion of **2'** and **3'**, is positioned 24.8 kcal/mol above **2'**. The calculated relative energies for **2'** and **3'**, as well as the magnitude of the barrier separating the two species (Scheme 4), are consistent with the observation that the O-bound carbonyl adduct is sufficiently long-lived to be observable, but is thermodynamically unstable. The considerably larger barrier for **2' → 3'** intramolecular nitromethanate rotation (24.8 kcal/mol), compared to that for **7' → 1'** ($\Delta G^\ddagger = 13.9$ kcal/mol), presumably reflects the coordinative saturation of the CO adducts.

Complexes **2'** and **3'** are both 18-e species with a monodentate H_2CNO_2 anion (O- and C-bound, respectively). **3'** is the thermodynamically more stable isomer by about 10 kcal/mol. This can be rationalized/predicted on the basis of the general rule that M–X and H–X bonds have similar relative bond energies,³⁷ and nitromethane is more stable than its nitronic acid tautomer by about 14 kcal/mol. The greater electronegativity of O versus C might be expected to favor the Ir–O-bonded isomer by more than 4 kcal/mol; however, this factor might be offset by Ir($d\pi$)–O($p\pi$) repulsive interactions present in **3'**.

Isomerization from the isocyanide bound, mono-oxygen-coordinated nitromethanate complex, **4**, to the carbon-coordinated nitromethyl complex **5** is analogous to the isomerization of complex **2** to **3**. Perhaps because of steric bulk of the cyclohexylisocyanide ligand, complex **4** is more labile than complex **2**. Electronic structure calculations, using methylisocyanide as a ligand rather than cyclohexylisocyanide, indicate that the O- to C-bound conversion is exothermic by approximately 10.0 kcal/mol ($\Delta G = 9.4$ kcal/mol), only about 1 kcal/mol less than the computed value in the CO case (complexes **2'** and **3'**). The calculated enthalpy of activation is 22.8 kcal/mol ($\Delta G^\ddagger = 23.5$ kcal/mol), also about 1 kcal/mol less than what was found in the CO case.

Conclusions

Pincer iridium nitromethanate complexes of three different binding modes were synthesized and characterized, within a single system. Reaction of (PCP)Ir with nitromethane forms the bidentate nitromethanate complex (PCP)Ir(H)(κ^2 -O,O-NO₂CH₂) (**1**). Reaction of **1** with CO affords the mono-oxygen-ligated nitromethanate CO adduct **2**, which is the first characterized transition metal mono-oxygen-ligated nitroalkane complex. An analogous reaction occurs with cyclohexylisocyanide to give mono-oxygen-ligated nitromethanate complex **4**. Upon heating, complexes **2** and **4** isomerize to give the carbon-ligated nitromethyl complexes **3** and **5**, respectively.

Computational studies indicate that the formation of complex **1** occurs via C–H oxidative addition to give a C-bound nitromethyl iridium hydride with weak Ir–O bonding. The (formally anionic) nitromethyl ligand can then rotate to give the κ^2 -O,O'-bound nitromethanate present in **1**. This appears to be the first reported example of oxidative addition of a C–H bond leading to a nitroalkane ligand.

Experimental Section

General Methods. Unless otherwise noted, all reactions, recrystallizations, and routine manipulations were performed at ambient temperature in an argon-filled glovebox or by using standard Schlenk techniques. Benzene and *p*-xylene were distilled from sodium/benzophenone under argon. Deuterated solvents for use in NMR experiments were dried as their protiated analogues, but were vacuum transferred from the drying agent. (PCP)IrH₂ was prepared according to published methods.³⁸ All other chemicals were used as received from commercial suppliers.

¹H and ³¹P{¹H} NMR spectra were obtained on a 300 MHz, Varian Mercury 300 spectrometer. ¹H NMR chemical shifts are reported in ppm downfield from tetramethylsilane and were referenced to residual protiated (¹H) solvents. ³¹P NMR chemical shifts are reported in ppm downfield from 85% H₃PO₄ and were referenced to external (capillary) PMe₃ in C₆D₆. Infrared (IR) spectra were recorded on an ATI Mattson Genesis Series FTIR in pentane or benzene solutions.

(PCP)Ir(H)(κ^2 -O,O-NO₂CH₂) (1). (PCP)IrH₂ (20 mg, 0.034 mmol) was dissolved in 2 mL of *p*-xylene solution containing 5.0 mg of norbornene (0.053 mmol) at room temperature. To the resulting solution was added 2.8 μL of nitromethane (0.052 mmol); after stirring for ca. 1 min, the red solution turned orange-yellow quickly. Solvent was evacuated and the resulting solid was redissolved in and recrystallized from pentane; yellow crystals were obtained (98% yield). ³¹P NMR (121.4 MHz, benzene-*d*₆): δ 59.16 (d, $J_{\text{PH}} = 12.8$ Hz). ¹H NMR (300 MHz, benzene-*d*₆): 6.85–6.92 (m, 3H, aromatic), 5.008 (s, 2H, CH₂), 23.233 (d of vt, $J_{\text{PH}} = 3.3$ Hz, $J_{\text{HH}} = 16.5$ Hz, 2H, CH₂), 2.948 (d of vt, $J_{\text{PH}} = 4.2$ Hz, $J_{\text{HH}} = 16.5$ Hz, 2H, CH₂), 1.433 (t, $J_{\text{PH}} = 6.3$ Hz, 18H, C(CH₃)₃), 1.296 (t, $J_{\text{PH}} = 6.3$ Hz, 18 H, C(CH₃)₃), –29.315 (t, $J_{\text{PH}} = 13.5$ Hz, 1H, Ir–H). ¹³C NMR (100.6 MHz, benzene-*d*₆): δ 148.9 (t, $J_{\text{CP}} = 8.2$ Hz, Ar C–Ir), 137.1 (s, Ar *o*-C), 137.0 (s, Ar *o*-C), 121.5 (s, Ar *p*-CH), 120.5 (vt, $J_{\text{CP}} = 7.6$ Hz, Ar *m*-CH), 100.1 (s, NO₂CH₂), 35.9 (vt, $J_{\text{CP}} = 9.2$ Hz, PC(CH₃)₃), 35.0 (vt, $J_{\text{CP}} = 9.2$ Hz, PC(CH₃)₃), 34.9 (vt, $J_{\text{CP}} = 14.0$ Hz, CH₂P), 29.5 (vt, $J_{\text{CP}} = 2.5$ Hz, PC(CH₃)₃), 29.3 (vt, $J_{\text{CP}} = 2.5$ Hz, PC(CH₃)₃). IR (pentane): $\nu_{(\text{C}=\text{N})} = 1575$ cm^{-1} , $\nu_{\text{as}(\text{NO}_2)} = 1181$ cm^{-1} , 1119 cm^{-1} , $\nu_{\text{s}(\text{NO}_2)} = 948$ cm^{-1} . Anal. Calcd for C₂₅H₄₆IrNO₃P₂: C, 46.40; H, 7.17; N, 2.17. Found: C, 46.32; H, 7.00; N, 1.95.

(PCP)Ir(H)(CO)(κ^1 -O-ONCOCH₂) (2). **1** (15 mg, 0.023 mmol) was dissolved in 2 mL of *p*-xylene. The solution was freeze–pump–thawed, and 800 Torr of CO was immediately added. The orange solution quickly turned yellow. Solvent was evaporated under reduced vacuum, and a pale yellow solid was obtained (95% yield). ³¹P NMR (121.4 MHz, benzene-*d*₆): δ 58.22 (d, $J_{\text{PH}} = 13.9$ Hz). ¹H NMR (300 MHz, benzene-*d*₆): 6.957 (t, $J_{\text{HH}} = 7.8$ Hz, 1H, aromatic), 6.852 (d, $J_{\text{HH}} = 7.8$ Hz, 2H, aromatic), 6.006 (s, 2H, CH₂), 2.996 (d of vt, $J_{\text{PH}} = 4.2$ Hz, $J_{\text{HH}} = 16.5$ Hz, 2H, CH₂), 2.924 (d of vt, $J_{\text{PH}} = 4.2$ Hz, $J_{\text{HH}} = 16.5$ Hz, 2H, CH₂), 1.379 (t, $J_{\text{PH}} = 7.05$ Hz, 18H, C(CH₃)₃), 1.212 (t, $J_{\text{PH}} = 6.6$ Hz, 18 H, C(CH₃)₃), –7.425 (t, $J_{\text{PH}} = 15.2$ Hz, 1H, Ir–H). ¹³C NMR (100.6 MHz, benzene-*d*₆): δ 184.8 (t, $J_{\text{CP}} = 6.8$ Hz, Ir–CO), 146.7 (t, $J_{\text{CP}} = 6.0$ Hz, Ar C–Ir), 133.9 (s, Ar *o*-C), 123.3 (s, Ar *p*-CH), 121.2 (vt, $J_{\text{CP}} = 7.3$ Hz, Ar *m*-CH), 93.4 (s, NO₂CH₂), 36.6 (vt, $J_{\text{CP}} = 14.1$ Hz, CH₂P), 35.7 (vt, $J_{\text{CP}} = 12.7$ Hz, PC(CH₃)₃), 35.3 (vt, $J_{\text{CP}} = 9.8$ Hz, PC(CH₃)₃), 29.3 (vt, $J_{\text{CP}} = 2.2$ Hz, PC(CH₃)₃), 28.7 (vt, $J_{\text{CP}} = 1.7$ Hz, PC(CH₃)₃). IR: $\nu_{(\text{CO})} = 2004$ cm^{-1} , $\nu_{(\text{C}=\text{N})} = 1547$ cm^{-1} . Anal. Calcd for C₂₆H₄₆IrNO₃P₂: C, 46.25; H, 6.87; N, 2.08. Found: C, 46.23; H, 6.87; N, 1.89.

(PCP)Ir(H)(CO)(CH₂NO₂) (3). **2** (15 mg, 0.023 mmol) was dissolved in 2 mL of *p*-xylene; the solution was then refluxed under

(37) Bryndza, H. E.; Fong, L. K.; Paciello, R. A.; Tam, W.; Bercaw, J. E. *J. Am. Chem. Soc.* **1987**, *109*, 1444–56.

(38) Zhu, K.; Achord, P. D.; Zhang, X.; Krogh-Jespersen, K.; Goldman, A. S. *J. Am. Chem. Soc.* **2004**, *126*, 13044–13053.

argon for 5 h. Solvent was evacuated, and the resulting solid was redissolved in and recrystallized from pentane; yellow crystals were obtained (90% yield). ^{31}P NMR (121.4 MHz, benzene- d_6): δ 50.08 (d, $J_{\text{PH}} = 6.0$ Hz). ^1H NMR (300 MHz, benzene- d_6): 6.96–7.06 (m, 3H, aromatic), 5.612 (t, $J_{\text{PH}} = 4.95$ Hz, 2H, CH_2), 3.104 (t, $J_{\text{PH}} = 7.5$ Hz, 4H, CH_2), 1.294 (t, $J_{\text{PH}} = 6.9$ Hz, 18H, $\text{C}(\text{CH}_3)_3$), 1.063 (t, $J_{\text{PH}} = 6.6$ Hz, 18H, $\text{C}(\text{CH}_3)_3$), -9.608 (t, $J_{\text{PH}} = 15.8$ Hz, 1H, Ir-H). ^{13}C NMR (100.6 MHz, benzene- d_6): δ 181.5 (t, $J_{\text{CP}} = 4.0$ Hz, Ir-CO), 147.3 (t, $J_{\text{CP}} = 5.6$ Hz, Ar C-Ir), 145.4 (s, Ar *o*-C), 123.8 (s, Ar *p*-CH), 120.5 (vt, $J_{\text{CP}} = 7.3$ Hz, Ar *m*-CH), 40.7 (vt, $J_{\text{CP}} = 14.5$ Hz, CH_2P), 36.9 (vt, $J_{\text{CP}} = 10.0$ Hz, $\text{PC}(\text{CH}_3)_3$), 36.2 (vt, $J_{\text{CP}} = 12.9$ Hz, $\text{PC}(\text{CH}_3)_3$), 32.9 (t, $J_{\text{CP}} = 4.5$ Hz, NO_2CH_2), 29.3 (s, $\text{PC}(\text{CH}_3)_3$), 28.6 (s, $\text{PC}(\text{CH}_3)_3$). IR: $\nu_{(\text{CO})} = 1988$ cm^{-1} , $\nu_{\text{as}(\text{NO}_2)} = 1498$ cm^{-1} , $\nu_{\text{s}(\text{NO}_2)} = 1355$ cm^{-1} . Anal. Calcd for $\text{C}_{26}\text{H}_{46}\text{IrNO}_3\text{P}_2$: C, 46.25; H, 6.87; N, 2.08. Found: C, 46.32; H, 6.78; N, 1.74.

(PCP)Ir(H)(cyclohexylisocyanide)(κ^1 -O-ONOCH₂) (4). Cyclohexylisocyanide (3.5 μL , 0.032 mmol) was added to a solution of 15 mg of **1** (0.023 mmol) in 2 mL of *p*-xylene, and the orange solution quickly turned pale yellow. Solvent was evaporated immediately under reduced vacuum, and a pale yellow solid was obtained (90% yield). ^{31}P NMR (121.4 MHz, benzene- d_6): δ 57.401 (d, $J_{\text{PH}} = 11.9$ Hz). ^1H NMR (300 MHz, benzene- d_6): 7.059–6.895 (m, 3H, PCP aromatic H), 5.964 (s, 2H, CH_2), 3.092 (d of vt, $J_{\text{PH}} = 3.9$ Hz, $J_{\text{HH}} = 15.6$ Hz, 2H, CH_2), 3.035 (d of vt, $J_{\text{PH}} = 3.9$ Hz, $J_{\text{HH}} = 15.6$ Hz, 2H, CH_2), 1.653–1.296 (m, 11H, cyclohexyl), 1.488 (t, $J_{\text{PH}} = 6.5$ Hz, 18H, $\text{C}(\text{CH}_3)_3$), 1.337 (t, $J_{\text{PH}} = 6.5$ Hz, 18H, $\text{C}(\text{CH}_3)_3$), -9.345 (t, $J_{\text{PH}} = 15.9$ Hz, 1H, Ir-H). ^{13}C NMR (100.6 MHz, benzene- d_6): δ 146.7 (t, $J_{\text{CP}} = 6.6$ Hz, Ar C-Ir), 141.1 (br, CN cyclohexyl), 138.3 (s, Ar *o*-C), 122.1 (s, Ar *p*-CH), 120.4 (vt, $J_{\text{CP}} = 6.9$ Hz, Ar *m*-CH), 92.8 (s, NO_2CH_2), 53.7 (s, CNCH cyclohexyl), 37.1 (vt, $J_{\text{CP}} = 13.5$ Hz, CH_2P), 35.5 (vt, $J_{\text{CP}} = 9.0$ Hz, $\text{PC}(\text{CH}_3)_3$), 35.4 (vt, $J_{\text{CP}} = 12.6$ Hz, $\text{PC}(\text{CH}_3)_3$), 32.3 (s, cyclohexyl C), 29.9 (vt, $J_{\text{CP}} = 2.2$ Hz, $\text{PC}(\text{CH}_3)_3$), 29.2 (vt, $J_{\text{CP}} = 1.7$ Hz, $\text{PC}(\text{CH}_3)_3$), 24.7 (s, cyclohexyl C), 23.5 (s, cyclohexyl C).

(PCP)Ir(H)(cyclohexylisocyanide)(CH₂NO₂) (5). Complex **4** isomerized to form complex **5** slowly. At room temperature, the isomerization was completed in 24 h. At 80 °C, the isomerization was completed within 2 h. Complex **4** (30 mg, 0.040 mmol) in *p*-xylene was heated at 80 °C for 2 h, solvent was evacuated, and the resulting solid was redissolved in and recrystallized from benzene as pale yellow crystals (90% yield). ^{31}P NMR (121.4 MHz, benzene- d_6): δ 47.293 (d, $J_{\text{PH}} = 7.29$ Hz). ^1H NMR (300 MHz, benzene- d_6): 7.058–6.997 (m, 3H, PCP aromatic H), 5.786 (t, $J_{\text{PH}} = 4.95$ Hz, 2H, CH_2), 3.302 (d of vt, $J_{\text{PH}} = 3.0$ Hz, $J_{\text{HH}} = 16.2$ Hz, 2H, CH_2), 3.191 (d of vt, $J_{\text{PH}} = 4.4$ Hz, $J_{\text{HH}} = 16.2$ Hz, 2H, CH_2), 1.643–1.296 (m, 11H, cyclohexyl), 1.410 (t, $J_{\text{PH}} = 6.5$ Hz, 18H, $\text{C}(\text{CH}_3)_3$), 1.206 (t, $J_{\text{PH}} = 6.2$ Hz, 18H, $\text{C}(\text{CH}_3)_3$), -11.729 (t, $J_{\text{PH}} = 16.7$ Hz, 1H, Ir-H). ^{13}C NMR (100.6 MHz, benzene- d_6): δ 150.5 (s, Ar *o*-C), 147.3 (t, $J_{\text{CP}} = 6.4$ Hz, Ar C-Ir), 137.4 (t, $J_{\text{CP}} = 5.2$ Hz, CN cyclohexyl), 122.6 (s, Ar *p*-CH), 119.7 (vt, $J_{\text{CP}} = 7.2$ Hz, Ar *m*-CH), 53.9 (s, CNCH cyclohexyl), 41.2 (vt, $J_{\text{CP}} = 14.3$ Hz, CH_2P), 37.1 (vt, $J_{\text{CP}} = 9.2$ Hz, $\text{PC}(\text{CH}_3)_3$), 35.9 (vt, $J_{\text{CP}} = 13.1$ Hz, $\text{PC}(\text{CH}_3)_3$), 34.1 (t, $J_{\text{CP}} = 3.9$ Hz, NO_2CH_2), 32.8 (s, cyclohexyl C), 29.8 (s, $\text{PC}(\text{CH}_3)_3$), 29.1 (s, $\text{PC}(\text{CH}_3)_3$), 24.5 (s, cyclohexyl C), 23.7 (s, cyclohexyl C). Anal. Calcd for $\text{C}_{32}\text{H}_{57}\text{IrN}_2\text{O}_5\text{P}_2$: C, 50.82; H, 7.60; N, 3.71. Found: C, 51.22; H, 7.73; N, 3.49.

Computational Details. For the electronic structure calculations we employed the DFT³⁹ method along with the PBE⁴⁰ exchange

and correlation functionals. The relativistic, small-core ECP and corresponding basis sets (split valence triple- ζ) of Dolg et al. were used for the Ir atom (SDD model).⁴¹ This 60-electron ECP releases the penultimate valence electrons (5s²5p⁶ for Ir) for explicit coverage by basis functions along with the valence electrons (6s²5d⁷). We used all-electron, full double- ζ plus polarization function basis sets for the second- and third-row elements C, N, O, and P (D95(d)).⁴² The hydrogen atom which formally becomes a hydride in the product complexes was described by the triple- ζ plus polarization 311G(p) basis set;⁴³ regular hydrogen atoms carried a double- ζ quality 21G basis set.⁴⁴

Reactant, transition state, and product geometries were fully optimized and the stationary points were characterized further by normal-mode analysis. The (unscaled) vibrational frequencies formed the basis for the calculation of vibrational zero-point energy (ZPE) corrections. Standard thermodynamic corrections were made to convert from purely electronic reaction or activation energies (ΔE , ΔE^\ddagger ; no ΔZPE) to enthalpies and free energies (ΔH , ΔH^\ddagger ; ΔG , ΔG^\ddagger ; ΔZPE included, $T = 298$ K, $P = 1$ atm).⁴⁵ To substantiate the nature of a particular transition state located, minimum energy paths were traced using the intrinsic reaction coordinate approach.⁴⁶ All calculations were executed using the GAUSSIAN 03 series of computer programs.⁴⁷

Our computational model for (PCP)Ir has methyl groups attached to the phosphorus atoms (i.e., $\text{PR}_2 = \text{P}(\text{CH}_3)_2$), a compromise between the use of hydrogen atoms and the bulky *tert*-butyl groups actually employed in the experimental systems. Methyl groups capture most of the electronic effects imparted by the *tert*-butyl groups, but they obviously do not fully model the steric bulk.^{48,49}

Acknowledgment. Financial support by the National Science Foundation (Grant CHE-0316575, and Grant CHE-0091872 for purchase of the Bruker SMART APEX diffractometer) is gratefully acknowledged.

Supporting Information Available: Crystallographic data for complexes **1**, **2**, **3**, and **5**. This material is available free of charge via the Internet at <http://pubs.acs.org>.

OM050659J

(41) Dolg, M.; Wedig, U.; Stoll, H.; Preuss, H. *J. Chem. Phys.* **1987**, *86*, 866.

(42) Dunning, T. H.; Hay, P. J. In *Modern Theoretical Chemistry*; Schaefer, H. F., III, Ed.; Plenum: New York, 1976; pp 1–28.

(43) Krishnan, R.; Binkley, J. S.; Seeger, R.; Pople, J. A. *J. Chem. Phys.* **1980**, *72*, 650.

(44) Binkley, J. S.; Pople, J. A.; Hehre, W. J. *J. Am. Chem. Soc.* **1980**, *102*, 939.

(45) McQuarrie, D. A. *Statistical Thermodynamics*; Harper and Row: New York, 1973.

(46) Schlegel, H. B.; Gonzalez, C. *J. Chem. Phys.* **1989**, *90*, 2154.

(47) Frisch, M. J.; Trucks, G. W.; Schlegel, H. B.; Scuseria, G. E.; Robb, M. A.; Cheeseman, J. R.; Montgomery, J. A., Jr.; Vreven, T.; Kudin, K. N.; Burant, J. C.; Millam, J. M.; Iyengar, S. S.; Tomasi, J.; Barone, V.; Mennucci, B.; Cossi, M.; Scalmani, G.; Rega, N.; Petersson, G. A.; Nakatsuji, H.; Hada, M.; Ehara, M.; Toyota, K.; Fukuda, R.; Hasegawa, J.; Ishida, M.; Nakajima, T.; Honda, Y.; Kitao, O.; Nakai, H.; Klene, M.; Li, X.; Knox, J. E.; Hratchian, H. P.; Cross, J. B.; Bakken, V.; Adamo, C.; Jaramillo, J.; Gomperts, R.; Stratmann, R. E.; Yazyev, O.; Austin, A. J.; Cammi, R.; Pomelli, C.; Ochterski, J. W.; Ayala, P. Y.; Morokuma, K.; Voth, G. A.; Salvador, P.; Dannenberg, J. J.; Zakrzewski, V. G.; Dapprich, S.; Daniels, A. D.; Strain, M. C.; Farkas, O.; Malick, D. K.; Rabuck, A. D.; Raghavachari, K.; Foresman, J. B.; Ortiz, J. V.; Cui, Q.; Baboul, A. G.; Clifford, S.; Cioslowski, J.; Stefanov, B. B.; Liu, G.; Liashenko, A.; Piskorz, P.; Komaromi, I.; Martin, R. L.; Fox, D. J.; Keith, T.; Al-Laham, M. A.; Peng, C. Y.; Nanayakkara, A.; Challacombe, M.; Gill, P. M. W.; Johnson, B.; Chen, W.; Wong, M. W.; Gonzalez, C.; Pople, J. A. *Gaussian 03*, Revision B.02; Gaussian, Inc.: Wallingford, CT, 2004.

(48) Wüllen, C. J. v. *J. Comput. Chem.* **1997**, *18*, 1985–1992.

(49) Cohen, R.; Rybtchinski, B.; Gandelman, M.; Rozenberg, H.; Martin, J. M. L.; Milstein, D. *J. Am. Chem. Soc.* **2003**, *125*, 6532–6546.

(39) Parr, R. G.; Yang, W. *Density-Functional Theory of Atoms and Molecules*; University Press: Oxford, 1989.

(40) Perdew, J. P.; Burke, K.; Ernzerhof, M. *Phys. Rev. Lett.* **1996**, *77*, 3865.